

# Unfolding of Titin Domains Explains the Viscoelastic Behavior of Skeletal Myofibrils

Ave Minajeva,\* Michael Kulke,\* Julio M. Fernandez,<sup>†</sup> and Wolfgang A. Linke\*

\*Institute of Physiology and Pathophysiology, University of Heidelberg, D-69120 Heidelberg, Germany; and <sup>†</sup>Department of Physiology and Biophysics, Mayo Foundation, Rochester, Minnesota 55905 USA

**ABSTRACT** The elastic section of the giant muscle protein titin contains many immunoglobulin-like domains, which have been shown by single-molecule mechanical studies to unfold and refold upon stretch-release. Here we asked whether the mechanical properties of Ig domains and/or other titin regions could be responsible for the viscoelasticity of nonactivated skeletal-muscle sarcomeres, particularly for stress relaxation and force hysteresis. We show that isolated psoas myofibrils respond to a stretch-hold protocol with a characteristic force decay that becomes more pronounced following stretch to above 2.6- $\mu$ m sarcomere length. The force decay was readily reproducible by a Monte Carlo simulation taking into account both the kinetics of Ig-domain unfolding and the worm-like-chain model of entropic elasticity used to describe titin's elastic behavior. The modeling indicated that the force decay is explainable by the unfolding of only a very small number of Ig domains per titin molecule. The simulation also predicted that a unique sequence in titin, the PEVK domain, may undergo minor structural changes during sarcomere extension. Myofibrils subjected to 1-Hz cycles of stretch-release exhibited distinct hysteresis that persisted during repetitive measurements. Quick stretch-release protocols, in which variable pauses were introduced after the release, revealed a two-exponential time course of hysteresis recovery. The rate constants of recovery compared well with the refolding rates of Ig-like or fibronectin-like domains measured by single-protein mechanical analysis. These findings suggest that in the sarcomere, titin's Ig-domain regions may act as entropic springs capable of adjusting their contour length in response to a stretch.

## INTRODUCTION

Elasticity is an inherent property of nonactivated striated muscle. The elements chiefly responsible for the elasticity have been shown to lie within the unitary structures of the muscle fibers, the sarcomeres, and to consist of titin (also called connectin) filaments (Wang, 1996; Maruyama, 1997; Linke and Granzier, 1998; Trinick and Tskhovrebova, 1999; Gregorio et al., 1999). A single titin molecule spans the length of a half-sarcomere, connecting the Z-line to the thick filaments (Fürst et al., 1988), but only the titin section located within the I-band region is functionally extensible. I-band titin exists in various-length isoforms expressed in different muscle types (Labeit and Kolmerer, 1995). Skeletal-muscle sarcomeres contain the N2-A isoform, whose extensible region comprises two main, structurally distinct, segments. One segment is the PEVK domain, a unique sequence with a high content of Pro (P), Glu (E), Val (V), and Lys (K), but no obvious secondary or tertiary structure. The PEVK domain is flanked on either side by a segment made up of serially linked immunoglobulin-like (Ig) domains, modules that fold into a seven-stranded  $\beta$ -barrel (Improta et al., 1996). The Ig-domain regions confer exten-

sibility to the sarcomere mainly at low stretch, the PEVK domain predominantly at higher stretch (Linke et al., 1996; Gautel and Goulding, 1996; Trombitas et al., 1998b).

The molecular basis of titin elasticity has been investigated in intact sarcomeres (e.g., Granzier et al., 1997; Trombitas et al., 1998a,b; Linke et al., 1998a,b) and on single isolated molecules (e.g., Rief et al., 1997; Tskhovrebova et al., 1997; Kellermayer et al., 1997; Carrion-Vazquez et al., 1999; Marszalek et al., 1999). The single-molecule studies first demonstrated that an entropic mechanism can explain the elasticity of titin. In these experiments, titin's force-extension relation could be readily simulated by a worm-like chain (WLC) model of polymer elasticity. The same model was then applied successfully to explain titin elasticity also in the bulk experiments. However, some controversial issues remained, particularly concerning the role of Ig domains. The analysis of titin extension in sarcomeres had indicated that titin's poly-Ig regions elongate on low stretch presumably by straightening out. Because these regions barely extend on higher stretch, it was proposed that individual Ig domains are unlikely to unfold, at least at physiologically relevant sarcomere extensions (Linke et al., 1996, 1998b; Trombitas et al., 1998b). In contrast, the single-molecule work suggested that Ig-domain unfolding is a probabilistic event. Therefore, unfolding should not occur only after a threshold force; rather, the probability of unfolding should continuously increase with the stretch force (Rief et al., 1998a; Fisher et al., 1999). Ig-domain unfolding should thus be present under physiological conditions (cf. Soteriou et al., 1993; Erickson, 1994). Clearly, this apparent discrepancy warranted closer examination.

Received for publication 29 August 2000 and in final form 27 November 2000.

A. Minajeva's permanent address: Department of Pathological Anatomy and Forensic Medicine, Tartu University, 50090 Tartu, Estonia.

Address reprint requests to Dr. Wolfgang A. Linke, Institute of Physiology and Pathophysiology, University of Heidelberg, Im Neuenheimer Feld 326, D-69120 Heidelberg, Germany. Tel.: 49-6221-544130; Fax: 49-6221-544049; E-mail: wolfgang.linke@urz.uni-heidelberg.de.

© 2001 by the Biophysical Society

0006-3495/01/03/1442/10 \$2.00

In the present study we reasoned that, if titin were a pure entropic spring, it should respond to an applied stretch in a truly elastic manner. However, we found that in the environment of the sarcomere, skeletal-muscle titin exhibits viscoelasticity, which manifests itself, for example, in stress relaxation (force decay at constant length) following a stretch and in force hysteresis during a stretch-release cycle. Such viscoelastic properties are observable already in slightly stretched isolated myofibrils. These observations prompted us to examine 1) whether the viscoelastic force response of nonactivated myofibrils is indeed likely to be derived from titin and 2) whether stress relaxation and force hysteresis may be explainable by unfolding and refolding of titin domains. Our main approach was to measure stress relaxation of myofibrils and to try to reproduce the force decay with a Monte Carlo simulation that takes into account the entropic elasticity of titin regions (including the PEVK region) as well as the unfolding characteristics of Ig domains established by single-molecule work. We also performed stretch-release experiments on relaxed myofibrils to investigate hysteresis and the time course of hysteresis recovery and then tried to relate the results to mechanical events known to take place in individual titin-Ig domains. The modeling indicated that the viscoelastic behavior of skeletal myofibrils at physiological sarcomere lengths (SLs) could arise from the unfolding/refolding of just a few Ig domains per titin molecule. In turn, we confirmed the absence of massive Ig-domain unfolding, consistent with the idea that skeletal-muscle titin principally behaves as an entropic spring (Linke et al., 1998a,b; Trombitas et al., 1998a,b). Whether a minor contribution to titin viscoelasticity also comes from some structural rearrangement of the PEVK domain, as suggested by the Monte Carlo simulation, remains to be seen. A model emerges in which titin's poly-Ig regions can be viewed as dynamic WLC elements capable of responding particularly to higher stretch forces with adjustment of their contour length. These findings help bridge the gap in explaining results from single-molecule work on titin versus those obtained in fiber stretch experiments.

## MATERIALS AND METHODS

### Myofibril mechanics

Myofibrils were isolated from freshly excised rabbit or rat psoas skeletal muscle as described (Linke et al., 1996). Briefly, thin muscle strips were dissected, tied to thin glass rods, and skinned in ice-cold rigor solution containing 0.5% Triton X-100 for  $\geq 4$  h. The skinned strips were minced and homogenized in rigor buffer. A drop of the suspension was placed on a coverslip on the stage of an inverted microscope (Zeiss Axiovert 135). Glass microneedles attached to a piezoelectric micromotor (Physik Instrumente, Waldbrunn, Germany) and a home-built force transducer (sensitivity,  $\sim 5$  nN; resonant frequency,  $\sim 700$  Hz), respectively, were then used to pick up small bundles containing two to eight myofibrils. To firmly anchor the specimen ends, the needle tips were coated with a silicone adhesive in a 1:1 (v/v) mixture of Dow Corning 3145 RTV and 3140 RTV. Water-

hydraulic micromanipulators (Narishige, Tokyo, Japan) were used to control the position of both needles. Experiments were performed at room temperature in relaxing solution of 200 mM ionic strength, pH 7.1 (Linke et al., 1997). Solutions contained 20 mM 2,3-butanedione monoxime to suppress any, possibly remaining, contractile activity. All solutions were supplemented with the protease inhibitor leupeptin to minimize titin degradation (Linke et al., 1998b).

### Data acquisition

Force data collection and motor control were done with a PC, data acquisition (DAQ) board (PCI-MIO-16-E1, National Instruments, Austin, TX), and custom-written LABVIEW software (Linke et al., 1998a,b). SL was measured either with a sensitive CCD camera (Völker, Maintal, Germany) and frame grabber board including image processing software (GlobalLab Image, Data Translation; Scion Image, based on National Institutes of Health Image, National Institutes of Health, Bethesda, MD) or by digitizing and analyzing the myofibril image, using a 2048-element linear photodiode array (Sony), the PC, DAQ board, and LABVIEW algorithms. Force data were stored in binary format and median-filtered off-line. If it was desirable to compare force data from different experiments, the force was related to cross-sectional area inferred from the diameter of the specimens as described (Linke et al., 1997).

### Experimental protocols

For the analysis of stress relaxation, specimens containing 2–5 myofibrils were pre-stretched to a desired SL above slack and were allowed to rest for a minimum of 10 min before being subjected to a ramp stretch, held isometrically for several seconds, and released quickly to the initial SL. The stretch amplitude was kept constant while the stretch speed was varied. Between measurements, a rest period of  $\sim 5$  min was observed. The protocol was performed at a series of different initial SLs. Sometimes, stress relaxation was also measured in myofibrils stretched to a number of different SLs from slack length. In control experiments, in which the motor needle was glued directly to the force transducer needle, we confirmed that the adhesive itself does not contribute to stress relaxation.

Hysteresis was investigated by subjecting slightly pre-stretched myofibrils to repetitive cycles of stretch-release (peak-to-peak amplitude, 0.1–0.2  $\mu\text{m}$ /sarcomere; frequency, 1 Hz). At the frequency chosen, the piezoelectric motor itself moved hysteresis-free. During measurements, both passive force and SL were recorded. The protocol was terminated normally after  $\sim 3$  min. Between measurements, the myofibril was released to slack length and care was taken to begin a new recording always after a fixed time delay following the re-stretch. Force traces were plotted and hysteresis was obtained by calculating the area enclosed by the stretch curve and release curve. To measure the time course of hysteresis recovery, a 25-ms stretch, 0.5-s hold, 10-ms release protocol was performed three consecutive times. Following each release step, a pause of varying duration was introduced.

### Stress relaxation fits

The stress relaxation data were tried to be fit by one-order, two-order, or three-order exponential decay functions. The latter, most frequently used function was of the following type:

$$f(t) = f_0 + A_1 \times \exp(-(t - t_0)/t_1) + A_2 \times \exp(-(t - t_0)/t_2) + A_3 \times \exp(-(t - t_0)/t_3), \quad (1)$$

where  $f_0$  and  $t_0$  are offset and center, respectively,  $A_1$  through  $A_3$  are decay amplitudes, and  $t_1$  through  $t_3$  are decay time constants. Curve fitting was

done by using a nonlinear least-squares method (Levenberg-Marquardt algorithm; Origin 5.0 software by Microcal, Amherst, MA).

## Monte Carlo simulations

Stress relaxation data were reproduced by a Monte Carlo technique based on entropic elasticity theory (WLC model) and the kinetic parameters of titin-Ig domain unfolding/refolding obtained in extension/relaxation experiments with single polyproteins (Carrion-Vazquez et al., 1999). Details of the Monte Carlo approach used by us were described previously (Rief et al., 1998a). The WLC model of entropic elasticity (Marko and Siggia, 1995) predicts the relationship between the relative extension of a polymer ( $z/L$ ) and the entropic restoring force ( $f$ ) through

$$f = (k_B T/A) [z/L + 1/(4(1 - z/L)^2) - 1/4], \quad (2)$$

where  $k_B$  is the Boltzmann constant,  $T$  is absolute temperature,  $A$  is the persistence length (a measure of the bending rigidity of the chain),  $z$  is the end-to-end length, and  $L$  is the chain's contour length. The modeling took into consideration the presence of unique sequence insertions in titin, mainly the PEVK segment, which acts as a (partly or completely) unfolded elastic region of several hundred nanometers length. The unique sequences were modeled as entropic springs behaving according to WLC theory (Eq. 2). Because the unique sequence insertions have a relatively short persistence length (Tskhovrebova et al., 1997; Linke et al., 1998a), the elastic properties of these regions dominate those of the entire titin chain (Kellermayer et al., 1997). A fixed value in the simulation was the number of Ig domains within the extensible section of one titin molecule, which is known to be 76 in rabbit psoas muscle (Freiburg et al., 2000).

In these Monte Carlo simulations, the force decay following a stretch was considered to be due to the unfolding of individual titin-Ig domains. As refolding is not observed in the presence of a force, the kinetics of domain refolding have no impact on the results of the simulation (Oberhauser et al., 1998; Carrion-Vazquez et al., 1999). However, external force greatly affects domain unfolding. The probability of observing the unfolding of any module  $P_u$  was calculated according to

$$P_u = (k_u^0 \times \Delta t) \times (\exp(f \times \Delta x_u / k_B T)), \quad (3)$$

where  $k_u^0$  is the Ig-domain unfolding rate at zero force,  $\Delta t$  is the polling interval,  $f$  is applied force, and  $\Delta x_u$  is the unfolding distance (Carrion-Vazquez et al., 1999). The simulations were performed in a LABVIEW (National Instruments) software environment. A feature of the custom-written software allowed selection of a desired number of iterations.

## RESULTS AND DISCUSSION

The force-extension relationship of titin in rat psoas myofibrils was simulated previously with a WLC model of entropic elasticity (Linke et al., 1998a,b). In that approach, the force per titin molecule was deduced from the quasi-steady-state force developed in nonactivated myofibrils at the end of a stretch-hold protocol. However, during the hold period following a stretch, myofibrils exhibit a typical force decline (Bartoo et al., 1997). This viscoelastic response, known as stress relaxation, was unexplained in earlier analyses of skeletal muscle elasticity (Linke et al., 1998a,b; Trombitas et al., 1998a,b), although titin has been proposed to contribute to the phenomenon (Wang et al., 1993; Higuichi, 1996). The present study was aimed at providing a possible theoretical explanation for the viscoelastic behavior of skeletal myofibrils.

## Characterization of stress relaxation in isolated myofibrils

To measure the stress relaxation response, bundles of two to three nonactivated rat psoas myofibrils were stretched from different initial SLs with constant amplitude but stretch speeds varying over three orders of magnitude. Specimens were held for 10 s at the stretched length before being released to the initial SL (Fig. 1 A). The magnitude of the viscoelastic force decay was recorded as well as the steady-state force (Fig. 1 B).

Force decay increased steadily with SL and stretch speed (Fig. 2, A–C). However, an exceptionally large decay amplitude was always noticeable following the quickest (4-ms) stretches. A major, distinct, fraction of that large decay ( $A_1$  in Fig. 1 C) was short-lived, lasting only 1–2 ms (Fig. 1 A, *inset*). The 1–2-ms component was absent when myofibrils were stretched more slowly, but following the 4-ms stretches it was present at all SLs, continuously increasing in magnitude above 3.0  $\mu\text{m}$  SL (Fig. 2 A, *dotted curve*). To

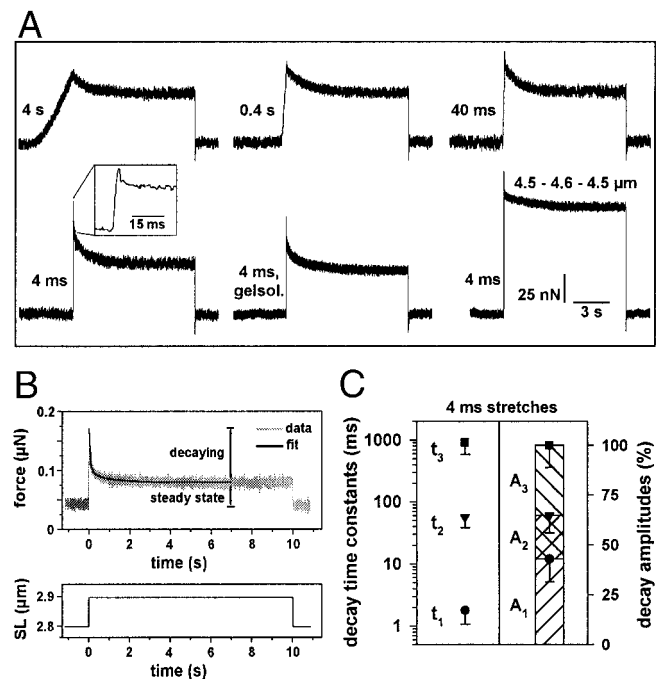
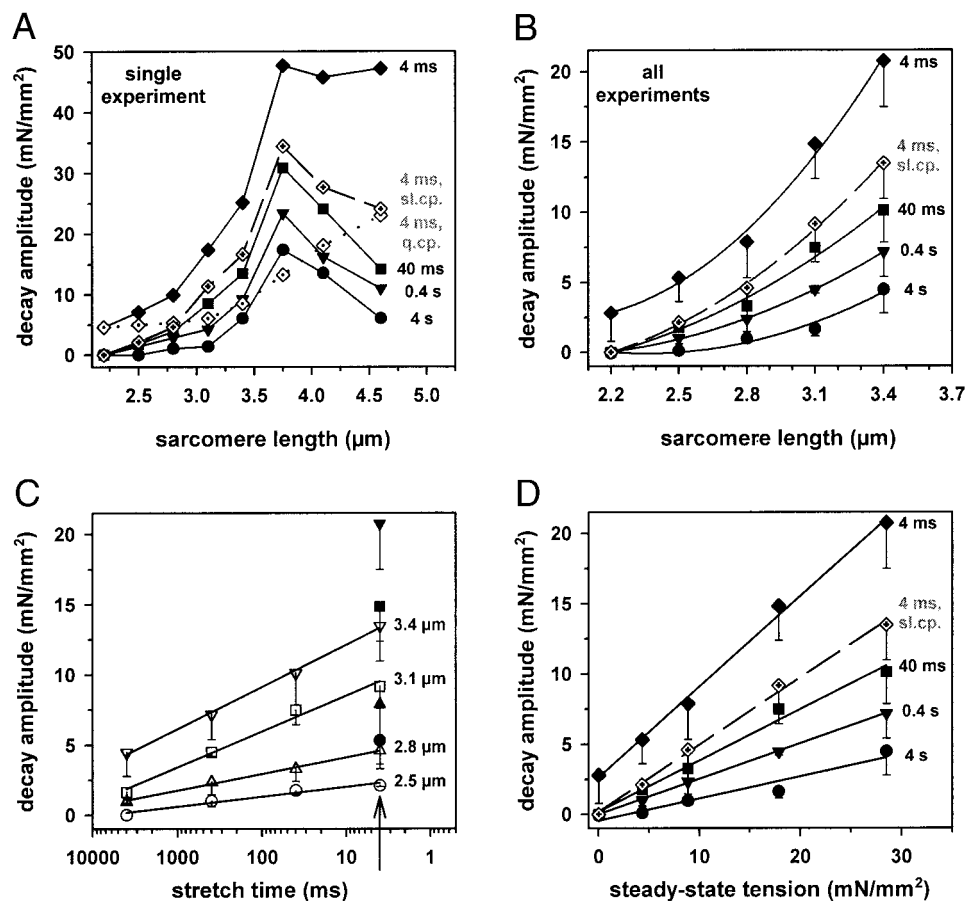


FIGURE 1 Force decay of myofibrils following stretches of constant amplitude (0.1  $\mu\text{m}$  per sarcomere) but variable stretch duration. (A) Representative force traces of a myofibril extended from 3.0  $\mu\text{m}$  initial SL to 3.1  $\mu\text{m}$  and released to 3.0  $\mu\text{m}$ , except the example in the bottom right panel, for which the protocol was 4.5 to 4.6 to 4.5  $\mu\text{m}$  SL. The time within which the stretch was completed is indicated in the panels. The force trace marked 4 ms, gelsol. was recorded after a 30-min exposure of the specimen to a calcium-independent gelsolin fragment (Linke et al., 1998a). (B) Stretch protocol and force response; the force decay after 4-ms stretches could be fit (nonlinear least-squares method) by a three-order exponential decay function (Eq. 1). (C) Results of fits of experimental data, obtained after 4-ms stretches of myofibrils to SLs between 2.8 and 3.1  $\mu\text{m}$ , to Eq. 1. The left panel shows the decay time constants (mean  $\pm$  SD;  $n = 10$ ), and the right panel the ratio between decay amplitudes (mean  $\pm$  SD;  $n = 10$ ).

FIGURE 2 Characterization of the viscoelastic force decay of psoas myofibrils. (a) Decay amplitude versus pre-stretch SL at different stretch durations, for one typical experiment. The curve labeled 4 ms, sl.cp. (— —) shows the decay amplitude after 4-ms stretch minus the short-lived decay occurring within the first 1.8 ms. The quickly decaying force (q.cp.) versus SL relation is also shown ( $\cdot \cdot \cdot$ ). (b) Force decay data from three different myofibrils at various SLs were averaged and are shown as mean  $\pm$  SD. Curves were fit by second-order regression. Shown separately is the slow component of force decay after 4-ms stretches (— —). (c) Plot of decay amplitude versus stretch duration (speed) at different SLs, from the data shown in b. Note logarithmic scale for stretch time. Data could be fit by simple regression, if only the slow component of force decay in the 4-ms stretch protocol was plotted (arrow). The whole decay amplitudes after 4-ms stretches are also shown (filled symbols). (d) Plot of decay amplitude versus steady-state tension at the end of the hold period. For all stretch speeds, data were fit by simple regression.



parameterize the decay time courses, we fit the force decline with exponential decay functions. A one-order exponential decay fit was sufficient to reproduce the stress relaxation response following the slowest stretches (4 s), whereas a two-order exponential decay function was appropriate to fit the force decline after 0.4-s and 40-ms stretches. Best results for the 4-ms stretch protocol were generally obtained with a three-order exponential decay fit (Fig. 1 B), which revealed time constants of  $1.8 \pm 0.7$  ms (mean  $\pm$  SD;  $n = 10$  at 2.8–3.1- $\mu$ m SL),  $56 \pm 18$  ms, and  $913 \pm 325$  ms (Fig. 1 C). The presence of a short-lived decay component was thus confirmed. Subtracting the short-lived component from the whole decay amplitude revealed a force decay versus SL relation (Fig. 2, A and B, *dashed curves*) more similar to that measured at slower stretch speeds. In a plot of decay amplitude versus log stretch speed, the data points at a given SL could now be fit by simple regression (Fig. 2 C). We hypothesize that the short-lived decay component is at least partly due to viscous drag arising from transient interactions between sarcomeric filaments and internal friction. Weakly attached actomyosin cross-bridges (Brenner et al., 1982) are unlikely to contribute much to the phenomenon, because the decay amplitude was barely reduced in myofibrils treated with a calcium-independent gelsolin fragment (Linke et al., 1998a) to extract actin (example in Fig. 1 A). Furthermore,

a large short-lived force decay was seen in myofibrils stretched to  $>3.8$ - $\mu$ m SL, i.e., beyond actin-myosin overlap (Fig. 1 A, *bottom right panel*; Fig. 2 A, *dotted curve*). In sum, the initial rapid force decay after quick stretching may include a truly viscous component, but the slower force decay may have a different source.

The forces measured in the small-scale myofibril preparation must originate in sarcomeric elements. Of these, the titin filaments (their elastic I-band sections) are known to determine steady-state force. Titin is thus a primary candidate to be considered also for the source of viscoelastic force decay. When we plotted force decay versus steady-state passive tension at the end of the hold period (Fig. 2 D), a linear relationship was found at all stretch speeds, supporting the idea that passive tension and viscoelastic decay have a common source, the titin filaments. The point is strengthened by the observation that force decay amplitude (excluding the short-lived component) rose to a maximum value at  $\sim 3.7$ - $\mu$ m SL but then declined at longer SLs (Fig. 2 A). Such a kind of curve shape has been described previously for the passive length-tension curve of psoas muscle fibers: the curve flattens or reverses near 4- $\mu$ m SL, because previously stiff A-band titin is recruited to the elastic titin portion (yield point) (Wang et al., 1991; Linke et al., 1996). Titin slippage at the thick filament anchor points on extreme

stretch may well be responsible for the decrease in force decay amplitude at very long SLs. Taken together, we conclude that, just as passive tension, stress relaxation of skeletal myofibrils may originate mainly in the titin molecules. This conclusion is consistent with that of previous mechanical analyses of resting whole skeletal muscle fibers (Mutungi and Ranatunga, 1996, 1998).

### Monte Carlo simulation of the stress relaxation response

The mechanical properties of titin-Ig domains have been investigated recently by atomic force microscopy (AFM) of polyproteins containing multiple copies of identical domains (Fisher et al., 1999). This has enabled the kinetic analysis of force-induced unfolding/refolding of individual titin-Ig modules, such as the I27 domain (Carrion-Vazquez et al., 1999), which locates to the region between PEVK segment and thick filament. Here we applied a Monte Carlo simulation taking into account the stretch force-dependent probability of I27 unfolding, together with the WLC model of entropic elasticity, to try to explain the time course of stress relaxation of skeletal myofibrils in terms of entropic-spring behavior of the titin segments and Ig-domain unfolding. At present it is not settled whether the mechanical stability of other Ig domains within the extensible I-band titin section is comparable to that of I27. A hint comes from AFM measurements of the mechanical stability of selected Ig domains from different I-band titin regions, which showed that the unfolding forces of these titin modules vary only slightly (Rief et al., 1998b). To address the issue of how a possible difference in Ig-domain stability might affect the force response to stretch, we varied the Ig-domain unfolding rate in the Monte Carlo model over a certain range.

The force data to be reproduced were obtained by stretching specimens containing three to four rabbit psoas myofibrils from slack length (mean,  $\sim 2.1\text{-}\mu\text{m}$  SL) to a series of longer SLs. After a hold period of 4–5 s, myofibrils were released to slack SL. Stretches and releases were completed within 40 ms, to avoid the appearance of a large short-lived decay component seen only after quicker stretches (cf. Figs. 1 and 2). A given protocol was repeated five times, and the force values were averaged. Fig. 3 shows the mean force (thick black lines) and experimental error (SD, gray areas) measured when a preparation was extended from  $2.17\text{ }\mu\text{m}$  to a series of longer SLs, here  $2.85\text{ }\mu\text{m}$  (Fig. 3 *a*),  $2.75\text{ }\mu\text{m}$  (Fig. 3 *b*), and  $2.65\text{ }\mu\text{m}$  (Fig. 3 *c*). The force data of Fig. 3 are representative of results obtained on four myofibrils.

Simulated force traces are indicated by the colored lines in Fig. 3. The stretch/release amplitudes were 340 nm (Fig. 3 *a*), 290 nm (Fig. 3 *b*), and 240 nm (Fig. 3 *c*), respectively, i.e., the amounts of stretch imposed on the elastic titin section of a half-sarcomere. Evidently, some simulations (to which noise was added to make them look more real) show

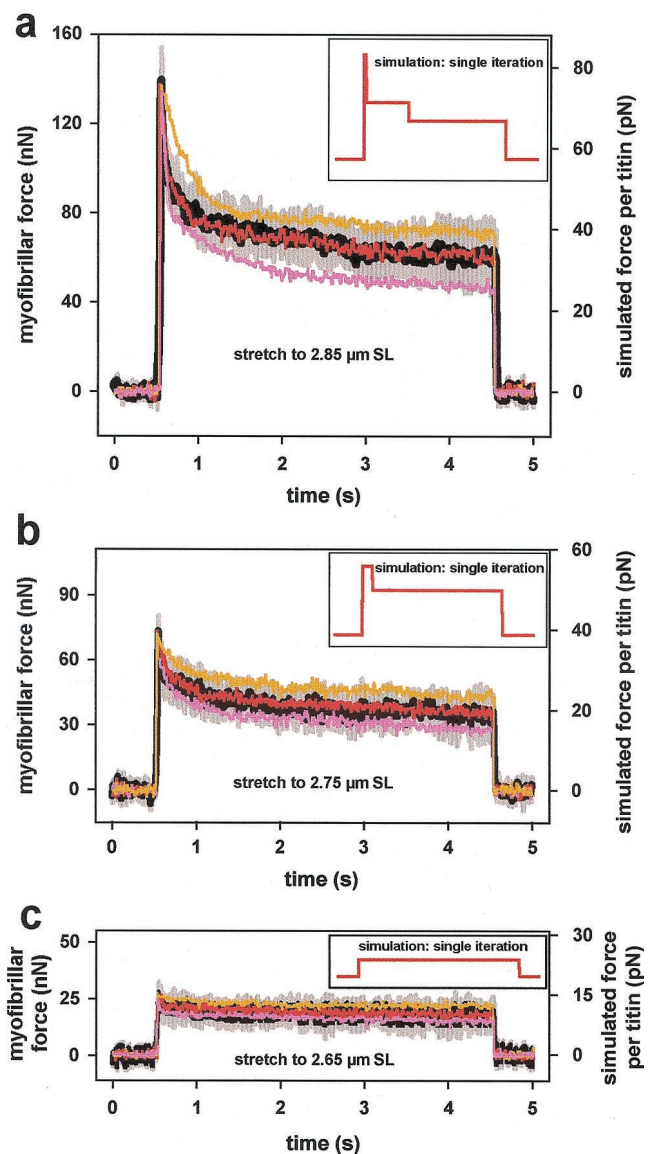


**FIGURE 3** Myofibrillar stress relaxation and Monte Carlo simulations. Myofibrils were stretched (stretch time, 40 ms) from the slack SL of  $2.17\text{ }\mu\text{m}$  and released (release time, 40 ms) to slack SL after a 4-s hold period. The black lines represent the mean of five measurements, gray areas are  $\pm$ SD. Force traces were reproduced by a Monte Carlo simulation based on Eqs. 2 and 3 (colored lines; average of 16 iterations, noise was added). The difference between the colored traces lies in the application of different unfolding rate constants: yellow trace,  $1 \times 10^{-4}\text{ s}^{-1}$ ; red trace,  $5 \times 10^{-4}\text{ s}^{-1}$ ; pink trace,  $9 \times 10^{-4}\text{ s}^{-1}$ . (Insets) Force traces of single iterations in the Monte Carlo simulation, indicating step-wise force decay. An unfolding rate constant of  $5 \times 10^{-4}\text{ s}^{-1}$  was used. In *a*,  $2.08 \pm 0.68$  (mean  $\pm$  SD;  $n = 200$  iterations) Ig domains per titin molecule were predicted to unfold on average, in *b*,  $1.27 \pm 0.62$  domains, and in *c*,  $0.24 \pm 0.49$  domains. For further details, see text.

striking similarity with the experimental data. The shape of the measured force responses could be reproduced faithfully (red curves in Fig. 3) by using values of 0.28 nm for the unfolding distance, 28.5 nm for the contour-length gain

upon unfolding of one Ig domain, and, most importantly,  $5 \times 10^{-4} \text{ s}^{-1}$  for the unfolding rate at zero force (cf. Carrion-Vazquez et al., 1999). We found that, for stretches up to at least  $3.0 \mu\text{m}$ , the longest SL investigated, any given force trace could be successfully simulated with the WLC model and the kinetic parameters of mechanically induced Ig-domain unfolding. To check an effect on the force decay possibly brought about by some diversity of Ig-domain stability, we applied unfolding rate constants (at zero force) that differed by almost an order of magnitude. In Fig. 3, the yellow and pink curves were obtained by using unfolding rates of  $1 \times 10^{-4} \text{ s}^{-1}$  and  $9 \times 10^{-4} \text{ s}^{-1}$ , respectively. Clearly, these curves do not follow the experimentally determined mean force decay particularly at longer SLs (Fig. 3, *a* and *b*). At the shorter SL (Fig. 3 *c*), the difference between the fit curves was less obvious. For even smaller stretches below  $\sim 2.6\text{-}\mu\text{m}$  SL, the stress relaxation response became negligible and the difference between fit curves disappeared almost completely (data not shown). In this context it is noted that unfolding of Ig domains is unlikely to take place also at intermediate SLs during quick myofibril stretch. Rather, from the mechanical properties of Ig domains it would be predicted that unfolding occurs after completion of the stretch (J. M. Fernandez, unpublished data). Altogether, the Monte Carlo modeling demonstrated that the stress relaxation response is readily explainable by unfolding of titin-Ig domains, if the unfolding characteristics previously established in single-molecule work on titin are taken into account.

### Involvement of the PEVK domain?

The simulation also proved to be quite sensitive to the actual numbers for persistence length  $A$  and contour length  $L$  of the pre-unfolded titin region, represented by the unique I-band titin sequences (i.e., mainly the PEVK domain). Good fits required some variation of these parameters. In the example of Fig. 3 *a*,  $L$  was set to 400 nm, which is reasonable for the unique sequences of rabbit psoas titin comprising  $\sim 1000$  residues (Freiburg et al., 2000) maximally spaced at 0.4 nm.  $A$  was set to 0.60 nm, which is the value predicted for the PEVK domain in a previous study (Linke et al., 1998a). In the example of Fig. 3 *b*,  $L = 360$  nm and  $A = 0.80$  nm; in Fig. 3 *c*,  $L = 345$  nm and  $A = 1.0$  nm. A decreased contour length and an increased persistence length at lower extension would be consistent with the proposal that some intramolecular bonds exist within titin's PEVK domain particularly at shorter SLs (Linke et al., 1998a; Trombitas et al., 1998b). Then, the possibility exists that minor structural changes occur within the PEVK domain during stretching (e.g., breakage of electrostatic bonds) (Linke et al., 1998a), which might add somewhat to titin's viscoelastic behavior. It remains to be seen whether the PEVK domain itself contributes to the stress relaxation of skeletal myofibrils. Another possibility is that interaction of PEVK-titin with

the thin filament (reported in preliminary form by Gutierrez et al., 1997) poses a viscous drag onto the sarcomere, resulting in some force decay after a stretch. One might also speculate that the short-lived component of force decay seen only after quick stretching (Figs. 1 and 2) could arise from the mechanical properties of the PEVK domain and/or from interactions involving PEVK-titin. In any case, some contribution of the PEVK domain to the stress relaxation phenomenon cannot be discounted at this stage. However, the striking reproducibility of the myofibrillar force decay by application of experimentally determined Ig-domain unfolding parameters led us to argue that the dominant factor for the viscoelastic force decay is the unfolding of Ig modules.

### How many titin-Ig domains may unfold during stress relaxation?

The Monte Carlo technique was also used to predict the number of Ig domains likely to unfold during stress relaxation. Two hundred iterations were generated arbitrarily (an unfolding rate constant of  $5 \times 10^{-4} \text{ s}^{-1}$  was generally assumed in these simulations), and the number of unfolding events in each iteration was counted. One unfolding event is seen as a distinct force step during the hold period (Fig. 3, *a-c*, insets). We point out that such a step-wise force decrease has been observed previously in single isolated titin molecules stretched and held with optical tweezers (Tskhovrebova et al., 1997). For a SL change from  $2.17 \mu\text{m}$  (slack SL) to  $2.85 \mu\text{m}$ , the Monte Carlo simulation predicted that, on average,  $\sim 2.1$  Ig domains per titin molecule unfold over a 4-s hold period (Fig. 3 *a*). Following stretch to  $2.75\text{-}\mu\text{m}$  SL and  $2.65\text{-}\mu\text{m}$  SL,  $\sim 1.3$  and  $\sim 0.25$  Ig domains/molecule, respectively, were predicted to unfold (Fig. 3, *b* and *c*). At stretch-hold below  $\sim 2.6\text{-}\mu\text{m}$  SL, the number of unfolding events dropped to near zero (data not shown). Thus, Ig-domain unfolding should practically be negligible in rabbit psoas myofibrils stretched between slack length and  $2.5\text{--}2.6\text{-}\mu\text{m}$  SL. It is precisely within this SL range that psoas titin elongates mainly by straightening out the Ig-domain segments (Linke et al., 1998b). At  $2.6\text{-}\mu\text{m}$  SL, the Ig-domain regions are extended by  $\sim 80\%$  of their contour length (at the same SL, the PEVK region stretches to  $\sim 20\%$  of its contour length (Linke et al., 1998a)), and only then may unfolding of individual Ig domains become practically relevant. In conclusion, the Monte Carlo modeling indicated that the viscoelastic force decay following stretch within a physiologically relevant range of SLs is not associated with massive Ig-domain unfolding. Instead, the force decay may reflect the unfolding of only a very small number of modules per titin molecule. Since perhaps 1000–2000 parallel titin molecules are present in the (half)-sarcomere of a myofibril, unfolding of one Ig domain per titin molecule would still add up to a significant number of unfolded modules in a muscle fiber.

### Force hysteresis during stretch-release

Another typical feature of viscoelasticity is force hysteresis, usually observable as higher force during stretch than during release. Force hysteresis has recently been described during stretch-release of single cardiac myocytes and has been proposed to originate in the titin molecules (Helmes et al., 1999). Furthermore, the amount of hysteresis was seen to drop greatly during repetitive (1.5-Hz) stretch-release cycles, indicating mechanical wearing-out of cardiac titin. The element in titin responsible for hysteresis and hysteresis adjustment was suggested by Helmes et al. to be an isoform-specific I-band segment expressed only in cardiac muscle (Labeit and Kolmerer, 1995): a 572-residue unique sequence with extensible properties (Linke et al., 1999). We argued that if this titin segment were the sole determinant of (adjustable) hysteresis, skeletal-muscle titin, which lacks that region, should exhibit the same force during stretch as during release. However, when isolated rabbit psoas myofibrils ( $n = 11$ ) were exposed to 1-Hz stretch-release cycles, we did find substantial force hysteresis. Fig. 4 shows representative examples. Unlike in cardiac cells, hysteresis mostly remained unchanged during repetitive measurements over a 3-min period (Fig. 4), although minor changes occurred in some specimens perturbed below  $\sim 3\text{-}\mu\text{m}$  SL. When myofibrils extended to  $>3\text{-}\mu\text{m}$  SL were stretched/released repetitively, a small drop of hysteresis was usually seen (Fig. 4), but the wearing-out was never as dramatic as in the cardiac myocytes. These results prompted us to take a closer look at the hysteresis of skeletal-muscle sarcomeres to try to associate the phenomenon with the mechanical properties of titin.

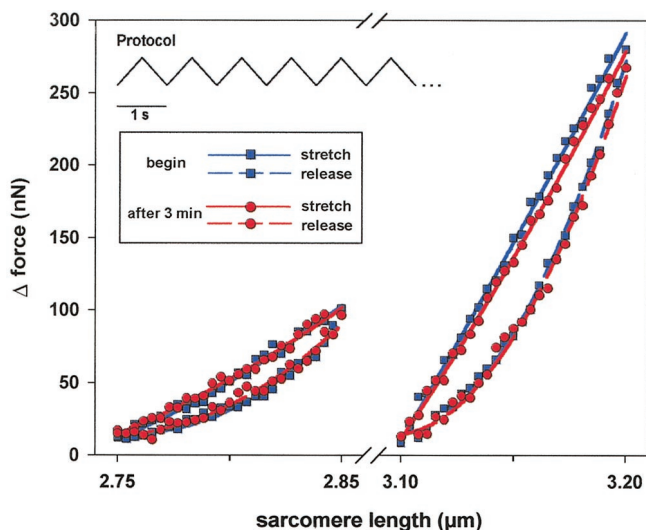


FIGURE 4 Example of force hysteresis in a myofibril stretched and released repetitively at two different SL ranges. Data points represent the force average of 10 cycles recorded at the beginning and at the end, respectively, of a 3-min measurement period. Fit curves are second-order regressions.

### Time course of hysteresis recovery

In a protocol designed to analyze hysteresis in more detail, small bundles of rabbit psoas myofibrils were stretched quickly from very low force levels, held for 0.5 s, and released to the initial length with highest motor speed. Following a pause of varying duration ( $\Delta t$ ), the cycle was repeated two more times (Fig. 5, protocol). The force response was usually similar in the second and third stretch, but depending on pause duration, force could be distinctly different in the first stretch (Fig. 5 *a*). The area under each stretch curve ( $A_s^1$ ,  $A_s^2$ , and  $A_s^3$ ) was calculated and any difference taken as a measure of incomplete hysteresis recovery. To determine the time course of hysteresis recovery, we measured the difference between  $A_s^1$  and  $A_s^2$  at a given  $\Delta t$  and expressed it relative to that obtained at  $\Delta t = 0$ .

Hysteresis  $h$  was found to recover with a double-exponential time course that could be fit by a nonlinear least-squares method (Levenberg-Marquardt algorithm) to the

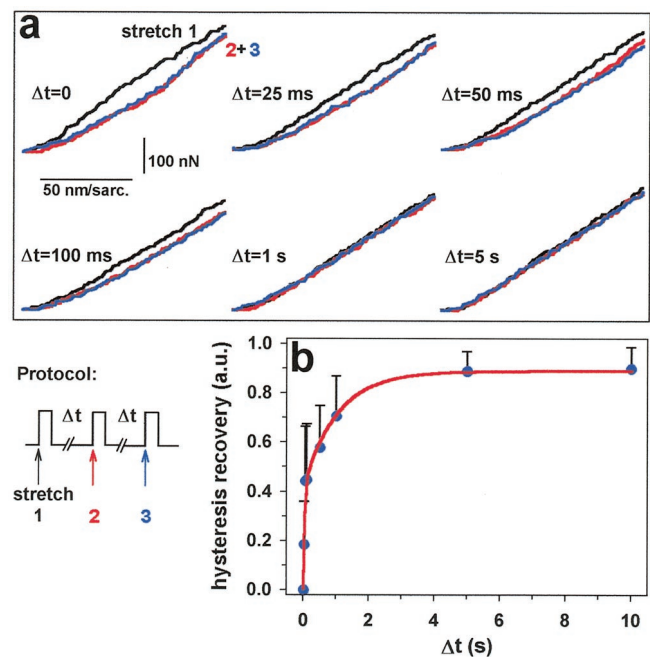


FIGURE 5 Recovery of force hysteresis of psoas myofibrils. Slightly pre-extended specimens were exposed three consecutive times to a rapid stretch, 0.5-s hold, rapid release protocol, while a pause of varying duration,  $\Delta t$ , was introduced following each release step. (*a*) In a typical experiment, the second and third stretch usually gave a similar force response. Force could also be similar in the first stretch, but only if pause duration was at least  $\sim 1$  s. With shorter pauses, the second/third stretch always resulted in lower force, indicating incomplete hysteresis recovery. This scenario would be expected if unfolding of Ig domains occurs after the first stretch but refolding is not complete before the second stretch commences. (*b*) Plot of hysteresis recovery, calculated as described in the text, versus pause duration. Hysteresis values are shown as mean  $\pm$  SD ( $n = 11$  myofibrils). Data points could be fit best by a two-exponential function (Eq. 4).

function

$$h_{\text{recov}} = a_1(1 - \exp(-\Delta t\beta_1)) + a_2(1 - \exp(-\Delta t\beta_2)), \quad (4)$$

where  $a_1 = 0.42 \pm 0.09$ ,  $a_2 = 0.47 \pm 0.09$ ,  $\beta_1 = 28 \pm 10 \text{ s}^{-1}$ , and  $\beta_2 = 1.0 \pm 0.4 \text{ s}^{-1}$  (Fig. 5 *b*). Hence,  $\sim 42\%$  of the recovery occurred at a fast rate of  $28 \text{ s}^{-1}$ , whereas  $\sim 47\%$  occurred at a slower rate of  $1 \text{ s}^{-1}$ . Remarkably, the slower recovery rate is quite similar to the refolding rate of the titin-Ig domain I27 ( $1.2 \text{ s}^{-1}$ ) measured by AFM (Carrion-Vazquez et al., 1999). It is not unlikely that the slower recovery process seen in our experiments may be due to the refolding of a subset of Ig domains in titin's I-band section. If so, we still do not know whether the hysteresis recovery reflects the refolding of I27 or that of other titin-Ig domains with similar mechanical properties. Because the I27 module locates to a titin segment shown to have somewhat lower extensibility than the more N-terminal Ig-domain segment next to the Z-disk (Gautel et al., 1996; Bennett et al., 1997; Linke et al., 1999), it is possible that the Ig modules from the latter region unfold preferentially. Elsewhere it was shown that the unfolding forces of selected Ig domains from the N-terminal segment barely differ from the unfolding force of I27 (Rief et al., 1998b). Thus, although a comparison was made here with the unfolding/refolding kinetics of I27, the conclusions of this study may bear more general significance.

The faster rate constant of hysteresis recovery ( $28 \text{ s}^{-1}$ ) compares well with that measured for the refolding of other modular domains with  $\beta$ -sheet fold, such as the 10th FNIII module of human fibronectin (fast refolding rate  $\sim 20 \text{ s}^{-1}$  (Plaxco et al., 1996)) and FNIII domains of tenascin (fast refolding rate  $42 \text{ s}^{-1}$  (Oberhauser et al., 1998)). Furthermore, it cannot be excluded that titin-Ig domains with similar sequence nevertheless differ in their unfolding rates; FNIII domains do show such diversity (Plaxco et al., 1997). Then, the fast rate constant of hysteresis recovery found here could reflect the refolding of an Ig-domain population in titin that has not yet been investigated by single-protein mechanics. In fact, assuming the presence of two Ig-domain sets with different mechanical behavior is not unreasonable, because sequence data suggest that the I-band titin repeats constitutively expressed in all muscle tissues (including I27) and those tissue-specifically expressed in skeletal muscles represent distinct subgroups (Witt et al., 1998). Alternatively, some I-band titin domains could refold in a biphasic process, like many fibronectin-like domains (Oberhauser et al., 1998), thus explaining the two-exponential recovery of force hysteresis in skeletal myofibrils. In any case, the time course of hysteresis recovery appears to be related to the refolding kinetics of titin-Ig domains.

A relatively fast time course of Ig-domain refolding ( $\geq 1 \text{ s}^{-1}$ ) also explains why hysteresis remained almost unchanged in psoas myofibrils stretched-released repetitively at a frequency of 1 Hz (Fig. 4). The fact that a similar

stretch-release protocol with cardiac myocytes did show decreased hysteresis (Helmes et al., 1999) may be due to a slow refolding of the unique 572-residue sequence present in cardiac titin only. Additionally, extrasarcomeric elements could contribute to slow hysteresis recovery of a cardiac cell. However, a significant part of the hysteresis recovery is fast also in cardiac myocytes (Helmes et al., 1999) and may represent the refolding of Ig domains. To conclude, hysteresis of skeletal myofibrils may arise from unfolding-refolding of a small number of Ig domains, in other words, from an adjustment of the contour length of titin's poly-Ig regions.

### Toward a synthesis

This study was initiated to address a major unresolved problem in current understanding of the molecular basis of titin elasticity, in particular concerning the role of Ig domains. Some time ago it was proposed that sarcomere extension involves unfolding of the  $\beta$ -sheet structure of Ig domains (e.g., Soteriou et al., 1993; Erickson, 1994). Subsequently it was shown in single-molecule AFM and optical tweezers studies that titin-Ig domains can be mechanically unfolded (Rief et al., 1997; Tskhovrebova et al., 1997; Kellermayer et al., 1997). The unfolding was considered to be a probabilistic event strongly dependent on the stretch forces acting on titin (Rief et al., 1998a; Fisher et al., 1999). In contrast, immunoelectron microscopic studies on intact sarcomeres concluded that in situ, the Ig-domain regions extend mainly by straightening and without the need to unfold individual modules; unique sequences (mainly the PEVK domain) were found to confer most of the extensibility to titin at modest to high physiological stretch (Linke et al., 1998a,b; Trombitas et al., 1998a,b).

The results of the present study now suggest a model in which unfolding of titin-Ig domains takes place in the sarcomere and underlies the force decay seen in isolated skeletal myofibrils during the hold period following a stretch (Fig. 3). Also the force hysteresis during stretch-release of myofibrils may be due to the unfolding/refolding of Ig domains, because the time course of hysteresis recovery is consistent with the kinetics of Ig-domain refolding (Fig. 5). Importantly, however, at physiologically relevant degrees of sarcomere stretch, only a few Ig domains per titin molecule may unfold; the vast majority of modules (more than  $\sim 97\%$ , depending on stretch amplitude) may remain folded. This could explain why immunoelectron microscopic analyses of titin extensibility have led to the conclusion that Ig-domain unfolding is no prominent feature of skeletal muscle elasticity (Linke et al., 1998b; Trombitas et al., 1998b). Unfolding of a couple of domains per titin molecule could easily be missed even by electron microscopy, because the unfolding of one domain, although it adds almost 30 nm to titin's contour length, will not result in a 30-nm increase in end-to-end length; because one unfolding event drops force dramatically by up to  $\sim 40\%$  (cf. Fig. 3 *a*,

*inset*), the unfolded domain will largely recoil. Along this line of reasoning we can explain both the results from the single-molecule work, which propose unfolding to occur as a probabilistic event, and those from experiments on intact sarcomeres, which suggest that, after initial straightening, Ig-domain regions are fairly stable segments.

Our findings, confirming the absence of massive Ig-domain unfolding, are consistent with the hypothesis that titin principally behaves as an entropic spring made up of serially linked WLCs with different bending rigidities: Ig-domain regions have a high bending rigidity (long persistence length) and extend before the PEVK domain (Linke et al., 1998a; Trombitas et al., 1998b). By suggesting that some Ig domains do unfold, the present study adds a new twist to this model. Domain unfolding has two important effects on protein elasticity: 1) it increases the protein's contour length and thus the range over which the protein can be extended, and 2) it decreases the persistence length, from that of a rigid chain of folded modules to that of a more flexible extended chain. Unfolding will therefore affect the entropic spring force and may be an efficient way to balance high external forces acting on a muscle fiber. Indeed, unfolding may become practically relevant only above a modest physiological SL, in psoas myofibrils  $\sim 2.6 \mu\text{m}$  (Fig. 3 c).

To sum up, titin filaments appear to be responsible for both elasticity and viscoelasticity of skeletal myofibrils. Monte Carlo simulations suggest that the viscoelastic behavior is likely to arise, to a large part, from the mechanical properties of titin's Ig-domain regions. Some contribution to viscoelasticity might also come from the PEVK domain of titin. However, stress relaxation, hysteresis, and hysteresis recovery of isolated psoas myofibrils were readily explained by the unfolding/refolding characteristics of individual Ig domains. In the sarcomere, Ig-domain regions may therefore act as entropic springs capable of adjusting their contour length in response to a stretch by unfolding of a very small number of modules per titin molecule.

The financial support of the Deutsche Forschungsgemeinschaft (Li 690/2-2; Li 690/5-1) is greatly acknowledged. JMF was supported by National Institutes of Health RO1 HL61228.

## REFERENCES

- Bartoo, M. L., W. A. Linke, and G. H. Pollack. 1997. Basis of passive tension and stiffness in isolated rabbit myofibrils. *Am. J. Physiol.* 273: C266–C276.
- Bennett, P. M., T. E. Hodkin, and C. Hawkins. 1997. Evidence that the tandem Ig domains near the end of the muscle thick filament form an inelastic part of the I-band titin. *J. Struct. Biol.* 120:93–104.
- Brenner, B., M. Schoenberg, J. M. Chalovich, L. E. Greene, and E. Eisenberg. 1982. Evidence for cross-bridge attachment in relaxed muscle at low ionic strength. *Proc. Natl. Acad. Sci. U.S.A.* 79:7288–7291.
- Carrion-Vazquez, M., A. F. Oberhauser, S. B. Fowler, P. E. Marszalek, S. E. Broedel, J. Clarke, and J. M. Fernandez. 1999. Mechanical and chemical unfolding of a single protein: a comparison. *Proc. Natl. Acad. Sci. U.S.A.* 96:3694–3699.
- Erickson, H. P. 1994. Reversible unfolding of fibronectin type III and immunoglobulin domains provides the structural basis for stretch and elasticity of titin and fibronectin. *Proc. Natl. Acad. Sci. U.S.A.* 91: 10114–10118.
- Fisher, T. E., A. F. Oberhauser, M. Carrion-Vazquez, P. E. Marszalek, and J. M. Fernandez. 1999. The study of protein mechanics with the atomic force microscope. *Trends Biol. Sci.* 24:379–384.
- Freiburg, A., K. Trombitas, W. Hell, O. Cazorla, F. Fougereousse, T. Centner, B. Kolmerer, C. Witt, J. S. Beckmann, C. C. Gregorio, H. Granzier, and S. Labeit. 2000. Series of exon-skipping events in the elastic spring region of titin as the structural basis for myofibrillar elastic diversity. *Circ. Res.* 86:1114–1121.
- Fürst, D. O., M. Osborn, R. Nave, and K. Weber. 1988. The organization of titin filaments in the half-sarcomere revealed by monoclonal antibodies in immunoelectron microscopy: a map of ten nonrepetitive epitopes starting at the Z-line extends close to the M-line. *J. Cell Biol.* 106: 1563–1572.
- Gautel, M., and D. Goulding. 1996. A molecular map of titin/connectin elasticity reveals two different mechanisms acting in series. *FEBS Lett.* 385:11–14.
- Gautel, M., E. Lehtonen, and F. Pietruschka. 1996. Assembly of the cardiac I-band region of titin/connectin: expression of the cardiac-specific regions and their relation to the elastic segments. *J. Muscle Res. Cell Motil.* 17:449–461.
- Granzier, H., M. Kellermayer, M. Helmes, and K. Trombitas. 1997. Titin elasticity and mechanism of passive force development in rat cardiac myocytes probed by thin-filament extraction. *Biophys. J.* 73:2043–2053.
- Gregorio, C. C., H. Granzier, H. Sorimachi, and S. Labeit. 1999. Muscle assembly: a titanic achievement? *Curr. Opin. Cell Biol.* 11:18–25.
- Gutierrez, G., A. van Heerden, J. Wright, and K. Wang. 1997. Titin elasticity: interaction and extensibility of PEVK segment of human fetal skeletal titin. *Biophys. J.* 72:A279.
- Helmes, M., K. Trombitas, T. Centner, M. Kellermayer, S. Labeit, W. A. Linke, and H. Granzier. 1999. Mechanically driven contour-length adjustment in rat cardiac titin's unique N2B sequence: titin is an adjustable spring. *Circ. Res.* 84:1339–1352.
- Higuchi, H. 1996. Viscoelasticity and function of connectin/titin filaments in skinned muscle fibers. *Adv. Biophys.* 33:159–171.
- Improta, S., A. Politou, and A. Pastore. 1996. Immunoglobulin-like modules from I-band titin: extensible components of muscle elasticity. *Structure.* 4:323–337.
- Kellermayer, M. S. Z., S. B. Smith, H. L. Granzier, and C. Bustamante. 1997. Folding-unfolding transitions in single titin molecules characterized with laser tweezers. *Science.* 276:1112–1116.
- Labeit, S., and B. Kolmerer. 1995. Titins, giant proteins in charge of muscle ultrastructure and elasticity. *Science.* 270:293–296.
- Linke, W. A., and H. Granzier. 1998. A spring tale: new facts on titin elasticity. *Biophys. J.* 75:2613–2614.
- Linke, W. A., M. Ivemeyer, S. Labeit, H. Hinssen, J. C. Rüegg, and M. Gautel. 1997. Actin-titin interaction in cardiac myofibrils: probing a physiological role. *Biophys. J.* 73:905–919.
- Linke, W. A., M. Ivemeyer, P. Mundel, M. R. Stockmeier, and B. Kolmerer. 1998a. Nature of PEVK-titin elasticity in skeletal muscle. *Proc. Natl. Acad. Sci. U.S.A.* 95:8052–8057.
- Linke, W. A., M. Ivemeyer, N. Olivieri, B. Kolmerer, J. C. Rüegg, and S. Labeit. 1996. Towards a molecular understanding of the elasticity of titin. *J. Mol. Biol.* 261:62–71.
- Linke, W. A., D. E. Rudy, T. Centner, M. Gautel, C. Witt, S. Labeit, and C. C. Gregorio. 1999. I-band titin in cardiac muscle is a three-element molecular spring and is critical for maintaining thin filament structure. *J. Cell Biol.* 146:631–644.
- Linke, W. A., M. R. Stockmeier, M. Ivemeyer, H. Hosser, and P. Mundel. 1998b. Characterizing titin's I-band Ig domain region as an entropic spring. *J. Cell Sci.* 111:1567–1574.
- Marko, J. F., and E. D. Siggia. 1995. Stretching DNA. *Macromolecules.* 28:8759–8770.

- Marszalek, P. E., H. Lu, H. Li, M. Carrion-Vazquez, A. F. Oberhauser, K. Schulten, and J. M. Fernandez. 1999. Mechanical unfolding intermediates in titin molecules. *Nature*. 402:100–103.
- Maruyama, K. 1997. Connectin/titin, giant elastic protein of muscle. *FASEB J.* 11:341–345.
- Mutungi, G., and K. W. Ranatunga. 1996. Tension relaxation after stretch in resting mammalian muscle fibers: stretch activation at physiological temperatures. *Biophys. J.* 70:1432–1438.
- Mutungi, G., and K. W. Ranatunga. 1998. Temperature-dependent changes in the viscoelasticity of intact resting mammalian (rat) fast- and slow-twitch muscle fibres. *J. Physiol.* 508:253–265.
- Oberhauser, A. F., P. E. Marszalek, H. P. Erickson, and J. M. Fernandez. 1998. The molecular elasticity of the extracellular matrix protein tenascin. *Nature*. 393:181–185.
- Plaxco, K. W., C. Spitzfaden, I. D. Campbell, and C. M. Dobson. 1996. Rapid refolding of a proline rich all  $\beta$ -sheet fibronectin type III domain. *Proc. Natl. Acad. Sci. U.S.A.* 93:10703–10706.
- Plaxco, K. W., C. Spitzfaden, I. D. Campbell, and C. M. Dobson. 1997. A comparison of the folding kinetics and thermodynamics of two homologous fibronectin type III modules. *J. Mol. Biol.* 270:763–770.
- Rief, M., J. M. Fernandez, and H. E. Gaub. 1998a. Elastically coupled two-level systems as a model for biopolymer extensibility. *Phys. Rev. Lett.* 81:4764–4767.
- Rief, M., M. Gautel, F. Oesterhelt, J. M. Fernandez, and H. E. Gaub. 1997. Reversible unfolding of individual titin immunoglobulin domains by AFM. *Science*. 276:1109–1112.
- Rief, M., M. Gautel, A. Schemmel, and H. E. Gaub. 1998b. The mechanical stability of immunoglobulin and fibronectin III domains in the muscle protein titin measured by atomic force microscopy. *Biophys. J.* 75:3008–3014.
- Soteriou, A., A. Clarke, S. Martin, and J. Trinick. 1993. Titin folding energy and elasticity. *Proc. R. Soc. Lond. B Biol. Sci.* 254:83–86.
- Trinick, J., and L. Tskhovrebova. 1999. Titin: a molecular control freak. *Trends Cell Biol.* 9:377–380.
- Trombitas, K., M. Greaser, G. French, and H. Granzier. 1998a. PEVK extension of human soleus muscle titin revealed by immunolabelling with the anti-titin antibody 9D10. *J. Struct. Biol.* 122:188–196.
- Trombitas, K., M. Greaser, S. Labeit, J.-P. Jin, M. Kellermayer, M. Helmes, and H. Granzier. 1998b. Titin extensibility in situ: entropic elasticity of permanently folded and permanently unfolded molecular segments. *J. Cell Biol.* 140:853–859.
- Tskhovrebova, L., J. Trinick, J. A. Sleep, and R. M. Simmons. 1997. Elasticity and unfolding of single molecules of the giant muscle protein titin. *Nature*. 387:308–312.
- Wang, K. 1996. Titin/connectin and nebulin: giant protein rulers of muscle structure and function. *Adv. Biophys.* 33:123–134.
- Wang, K., R. McCarter, J. Wright, J. Beverly, and R. Ramirez-Mitchell. 1991. Regulation of skeletal muscle stiffness and elasticity by titin isoforms: a test of the segmental extension model of resting tension. *Proc. Natl. Acad. Sci. U.S.A.* 88:7101–7105.
- Wang, K., R. McCarter, J. Wright, J. Beverly, and R. Ramirez-Mitchell. 1993. Viscoelasticity of the sarcomere matrix of skeletal muscles: the titin-myosin composite filament is a dual-stage molecular spring. *Biophys. J.* 64:1161–1177.
- Witt, C. C., N. Olivieri, T. Centner, B. Kolmerer, S. Millevoi, J. Morell, D. Labeit, S. Labeit, H. Jockusch, and A. Pastore. 1998. A survey of the primary structure and the interspecies conservation of I-band titin's elastic elements in vertebrates. *J. Struct. Biol.* 122:296–215.